ICASSP 2021 - 2021 IEEE International Conference on Acoustics, Speech and Signal Processing (ICASSP) | 978-1-7281-7605-5/20/$31.00 ©2021 IEEE | DOI: 10.1109/ICASSP39728.2021.9414167

A Bayesian Inference Approach for Location-Based Micro Motions using Radio Frequency Sensing

David A. Maluf*, Amr Elnakeeb†, Matt Silverman*
*Cisco Systems, San Jose, CA, USA
†University of Southern California, Los Angeles, CA, USA
*{dmaluf, masilver}@cisco.com, †{elnakeeb}@alumni.usc.edu

***Abstract*—The Bayesian inference is leveraged for target tracking from radio signals collected from access points (APs). The density of the moving object as well as its distance from the transmitted wireless signal substantially affect the signal strength arriving at the receiving end. The target tracking objective is formulated as an inference problem, by which we show how the Bayesian framework can be exploited to infer the parameters of interest for a given physics model. The channel state information (CSI) is collected from wireless APs, on which the inference is carried out. We employ a non-linear forward physics model of propagation, where we differentially infer the location, the velocity, and the fractional area of the moving surfaces in 3D space, versus time. The optimization is conducted via a Levenberg–Marquardt algorithm with analytically derived Jacobian and prior. The proposed model easily scales for any given number of access points. Experiments are conducted on Cisco wireless 4800 Access Point series; operating at 5 GHz radio frequency, and the probabilistic results for position and effective surface area estimates are provided, as well as numerical results for the point spread function from the statistics of the surface location.**

***Index Terms*—Bayesian inference, tracking, CSI, Access Points, gradient descent.**

I. Introduction

The proliferation of wireless devices has enabled location-based services (LBS) that eased our everyday life in many aspects, e.g., navigation, healthcare, entertainment [1–4]. For instance, accurate locations can be provided by the Global Positioning System (GPS) using smart phones; however, the performance of the GPS is substantially degraded in indoor environments [5]. To that end, numerous research works have focused on improving the performance of indoor LBS applications [5, 6]. For indoor applications, localization can be divided into two categories, namely device-based and device-free. Device-free localization must establish the nature of the target. In this paper, the target is any motion with the additional characteristic of surface area besides the location.

To derive a motion in free space, we consider first the state of the art in radio-based localization. In general localization research works are mainly classified into two categories: Range-based schemes [7–11] and range-free schemes [12–15]. Range-based schemes estimate the target's position by triangulation or trilateration, given the estimated distance between the target and at least three reference points. In this category, the distance is usually estimated from the wireless signal information, i.e., Time of Arrival (ToA), Time of Flight (ToF), and Received Signal Strength Indication (RSSI) [7–11]; however, each of the aforementioned parameters has an impediment. For instance, ToA and ToF suffer from time sensitivity; thus, requiring highly synchronized timers, which is rarely available in practice [7, 8]. Furthermore, the state-of-the-art is limited to line of sight (LOS) radio signals [7, 8] discarding multipath signals. Motion is therefore limited to devices only. These methods did not consider device-free body motion localization which is also captured by multipath effects. The indoor RSSI temporal and spatial fluctuations render the RSSI information not as useful as it is expected to be, when considering only device-based localization [9–11].

The multipath is further discarded in most of the range-free schemes focusing only on device-based localization, versus device-free body targeting. In particular, range-free schemes span vector hop (DV-hop) methods [13], proximity detection methods [12], and Angle of Arrival (AoA)-based methods [14, 15]. In DV-hop methods [13], the number of hops, among sensors, is leveraged to estimate the distance, given the prior knowledge of the exact locations of a few sensors, usually known as "anchor sensors." For proximity detection methods [12], Bluetooth low energy beacons are used to broadcast their locations periodically. Mobile devices in the neighborhood capture the signals of those beacons, and thus, the distances to the beacon are accordingly estimated. However, these methods require the deployment of a massive number of beacons for accurate estimation results. In AoA-based methods, they rely on two received AoAs and the locations of their receivers.

In the context of wireless localization, RSSI is easily obtainable, therefore, it is commonly used. However, as previously mentioned, it requires a LOS communication, which is not guaranteed, especially in indoor environments; the application that is considered in this work. Channel State Information (CSI) estimates the channel, on each subcarrier, in the frequency domain, thus, it better suits for multipath environments and Non-Line of Sight (NLoS) communication—unlike RSSI, that gives an aggregated value of all of the subcarriers' amplitudes [16, 17]. In this work, the CSI is used in a range-based environment, which is exclusively constructed of the multipath signals.

Bayesian framework has been successfully exploited for a variety of inference problems, due to its high estimation accuracy from noisy or incomplete data [18–21]. In addition, the Bayesian framework provides an estimate of the errors associated with the parameters being inferred, that can be exploited if the inference is carried out with time, to subsequently minimize the error [20, 21].

Bayesian framework refers specifically to physics-based models that need to be infered. In a nutshell, the ground truth is encapsulated in the model and not by comparing an output to another set of observations. Bayesian inference is the optimization-based search method for the solution in physics-based models. For example, it is used in astronomy to infer to characteristics of a phenomenon in space to check whether the data converges to the physical model or not [20, 21]. The physics model of choice in this paper is a derived subset from the radio propagation, and has been validated in ideal settings. The noise in real world setting is then minimized by the Bayesian inference itself once the nature of the noise

is known.

Intentionally, the selection of Bayesian as the inference method is that the localization physical phenomena are Gaussian in nature. The table below describes three well-known approaches to signal processing

In the context of target tracking; herein, the proposed model is a parameterized signal strength model, from which synthetic observations are generated. The proposed model performs rendering, a common term in computer vision and computer graphics [22] and is used in this paper to underline the generalization in nature of optics. None of the prior art has considered the incorporation of physical and mathematical models that nearly fit the nature of the collected measurements using Bayesian principles. This work falls in the same category with the work considered in [20, 21] at NASA. For different radio frequencies, different physical-propagation laws apply. For the case of wireless signals, we demonstrate how the moving micro surface areas, diffuse coefficients, locations and velocities can be inferred, based on the proposed model. The contributions of this work are summarized as follows:

1) A Bayesian framework is proposed for the surface tracking objective.
2) The resulting optimization problem, in which a non-linear forward model is linearized, is solved via gradient descent methods.
3) The location of the moving surface, the fractional area and the diffuse reflection coefficient as well as the velocity are inferred, versus time.

II. Proposed Model

We assume that the transmitter is an isotropic source, and the signal is reflected via the object surface, that follows Lambertian reflectance [20], and then arrives at the receiving radio end. The Lambertian reflectance model for indoor environments is given in [23]. We follow the free space attenuation model [24]; that is, the received power at the receiving antenna is given by,

$$P_{RX} = \frac{A_{RX}}{4\pi R^2} P_{TX}, \tag{1}$$

where P_{TX} is the power reflected (transmitted) by the surface, A_{RX} is the effective area of the receiving antenna, and R is the distance between that object (surface) and the receiving end. In terms of electric field strength [25],

$$P_{RX} = \frac{|E_r|^2}{Z_0} A_{RX}, \text{and} \tag{2}$$

$$P_{TX} = \frac{|E_s|^2}{Z_0} \rho A_e, \tag{3}$$

where, $|E_r|$ and $|E_s|$ are the magnitude of the electric field strength at the receiving and transmitting ends, respectively. Further, A_e denotes the effective area of the object, Z_0 is the impedance of free space; $Z_0 = 120\pi\Omega$, and ρ is the albedo. In other words, ρA_e denotes the effective surface area of the object. Substituting from Equations (2) and (3) into Equation (1) yields,

$$|E_r| = \frac{\sqrt{\rho A_e}}{2\sqrt{\pi} R} |E_s|. \tag{4}$$

Define the normalized magnitude of electric field strengths as M, where,

$$M = \frac{|E_r|}{|E_s|} = \frac{\sqrt{\rho A_e}}{2\sqrt{\pi} R}. \tag{5}$$

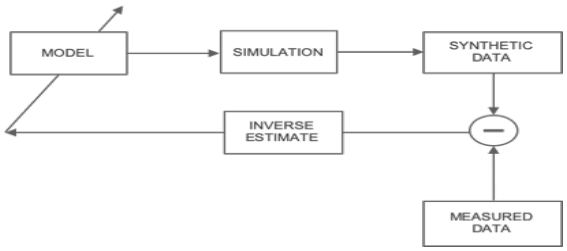

Fig. 1. Signal model.

Algorithm 1 : Phase Unwrapping Algorithm

Input: Measured (wrapped) phase ψ_l of L OFDM subcarriers; $l = 1, 2, \ldots, L$.
Output: Unwrapped phase ϕ_l of L OFDM subcarriers.
Initialization: Initialize $\phi_l = \psi_l, d = 0$.
for $l = 2 : L$ **do**
    If $\psi_l - \psi_{l-1} > \pi$ **then** $d = d + 1$
    $\phi_l = \psi_l - 2\pi d$
end for

Furthermore, the phase difference between the received and transmitted electric field is defined as,

$$\psi = \psi_{E_r} - \psi_{E_s}, \tag{6}$$

where ψ_{E_r} and ψ_{E_s} are the electric field phase at the receiving and transmit ends, respectively.

The measured phase is folded/wrapped due to the recurrence characteristic of phase. Therefore, the measured phase has to be transformed into the true "unwrapped" value. Algorithm 1 shows how the phase is unwrapped across the OFDM subcarriers (which will be used in this context); it is an adapted version of the algorithm presented in [14]. Then, we write the difference between the unwrapped phases as follows,

$$\phi = \phi_{E_r} - \phi_{E_s} = -\frac{2\pi}{\lambda}(2R) = -\frac{4\pi}{\lambda} R, \tag{7}$$

where, λ is the operating wavelength; $\lambda = \frac{c}{f}$ where c is the speed of light and f is the frequency of operation.

We consider a non-linear forward model, where we differentially infer the parameters of interest. Fig. 1 shows the general approach used herein. The synthetic observations are generated from the proposed model via computer simulations of the observation process via Equation (5), which are compared to the real measurements—herein, they represent the OFDM Channel State Information (CSI) measurements collected from multiple access points. The error between the real measurements and the synthetic observations is fed to the simulator, through which the system parameters are accordingly adjusted, to minimize the error in the subsequent instances of time. Put differently, the estimation of the errors means the system parameters are updated whenever more measurements are available.

III. Bayesian Framework and Proposed Algorithm

We consider a Bayesian framework for target tracking. The object of interest has an effective surface area ρA_e, and is located at distance R_i from the i-th access point, $i = 1, 2, \ldots, N$, where N denotes the total number of access points. We assume that not all matter moves at once, and for an infinitesimal period of time, motion is characterized by a

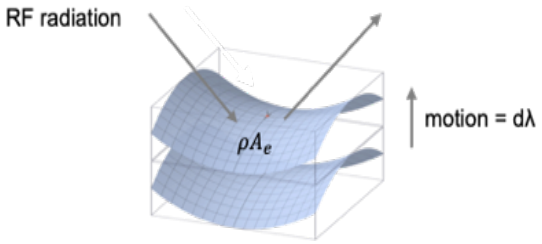

Fig. 2. Motion model.

fractional effective surface ρA_e that has moved a distance $d\lambda$, as shown in Fig. 2.

We seek estimation of the fractional area of the moving surfaces ρA_e, and the distances to each access point R_i, from which we directly estimate the location of the surface in space. The full vector of distances and differential surface area is defined as,

$$\mathbf{u} = [R_1, R_2, \ldots, R_N, \bar{A_e}] \in \mathbb{R}^{N+1}, \tag{8}$$

where, $\bar{A_e} = \rho A_e$. To estimate $\mathbf{u}$ from the collected measurements, we apply Bayes theorem [26]; that is,

$$p(\mathbf{u}|dM_1, \ldots, dM_N) \propto p(dM_1, \ldots, dM_N|\mathbf{u})p(\mathbf{u}), \tag{9}$$

where, dM_i; $i = 1, 2, \ldots, N$, is the differential component of the magnitude of the signal strength on the i-th access point. Equation (9) states that the posterior of the distances and differential surface area is proportional to the likelihood-the probability of observing the data given the distance and the surface area-multiplied by the prior distribution of the distances and surface area. Furthermore, the prior distribution is assumed to be zero-mean Gaussian, that is,

$$p(\mathbf{u}) \propto \exp\left(-\frac{1}{2}\mathbf{u}\mathbf{\Sigma}^{-1}\mathbf{u}^T\right), \tag{10}$$

where $\mathbf{\Sigma}^{-1} \in \mathbb{R}^{N+1 \times N+1}$ is the inverse covariance matrix,

$$\mathbf{\Sigma}^{-1} = \frac{4\pi}{\lambda}\begin{bmatrix} \chi_1 & 0 & \ldots & 0 & 0 \\ 0 & \chi_2 & \ldots & 0 & 0 \\ \vdots & \vdots & \ddots & \vdots & \vdots \\ 0 & 0 & \ldots & \chi_N & 0 \\ 0 & 0 & \ldots & 0 & 1 \end{bmatrix}, \tag{11}$$

which is designed, as in Equation (11), to reflect the physical layout among the antennae of each AP. For example, for an array of antennae, the distances given an array of antennae will vary relatively to their angle of arrivals. We penalize over the average difference, on each access point, between the differential distances dR_{ij} and the phase shifts $\frac{\lambda}{4\pi}d\phi_{ij}$ from the angles of arrival,

$$\chi_i = \frac{1}{\binom{V_i}{2}}\sum_{\substack{k,j \\ k \neq j}}^{\binom{V_i}{2}}\left(dR_{kj_i} - \frac{\lambda}{4\pi}d\phi_{kj_i}\right)^2, \tag{12}$$

where k, j denote two antennas' indices on any particular access point i; $i = 1, 2, \ldots, N$, and $\binom{V_i}{2}$ is the combination operator, i.e., V_i choose 2. Furthermore, V_i denotes the number of antennas on the i-th access point. If all access points have the same number of antennas, then $V_i = V$.

For the likelihood derivations, we make the following assumptions,

A1) The difference between the measured real data and the synthesized observed data follows a zero mean Gaussian distribution [20, 21].

A2) The measurements are conditionally independent.

Combining assumptions A1) and A2) yields,

$$p(dM_1, \ldots, dM_N|\mathbf{u}) \propto \exp\left(-\frac{\sum_{i=1}^{N}\left(dM_i - \hat{m}_i(\mathbf{u})\right)^2}{2\sigma^2}\right), \tag{13}$$

where, $\hat{m}_i(\mathbf{u})$ denotes estimated differential magnitude on the i-th AP, and σ^2 is the noise variance. Therefore, the negative-log posterior is written as,

$$\mathcal{L}(\mathbf{u}) \propto -\frac{\sum_{i=1}^{N}\left(dM_i - \hat{m}_i(\mathbf{u})\right)^2}{2\sigma^2} + \mathbf{u}\mathbf{\Sigma}^{-1}\mathbf{u}^T. \tag{14}$$

As can be clearly seen, Equation (14) is a nonlinear function of $\mathbf{u}$; and the MAP estimate is that value of $\mathbf{u}$ which minimizes $\mathcal{L}(\mathbf{u})$. Gradient methods can be applied to minimize negative log-posterior [20, 21, 27]. The vector of synthesized magnitudes of the motion is denoted by $\hat{\mathbf{m}}(\mathbf{u})$, which is linearized about the current estimate, that is,

$$\hat{\mathbf{m}}(\mathbf{u}) = \hat{\mathbf{m}}(\mathbf{u}_0) + \mathbf{D}(\mathbf{u} - \mathbf{u}_0), \tag{15}$$

where $\mathbf{D} \in \mathbb{R}^{N \times N+1}$ is the matrix of derivatives evaluated at $\mathbf{u}_0$. The i-th row of $\mathbf{D}$ is given by $\left[\frac{\partial \hat{\mathbf{m}}_i(\mathbf{u})}{\partial R_j}, \frac{\partial \hat{\mathbf{m}}_i(\mathbf{u})}{\partial A_e}\right]$, with $i, j = 1, 2, \ldots, N$. Thus, $\mathbf{D}$ is written as,

$$\mathbf{D} = \begin{bmatrix} -\frac{\sqrt{\bar{A_e}}}{R_1^2} & \frac{\sqrt{\bar{A_e}}}{R_1 R_2} & \ldots & \frac{\sqrt{\bar{A_e}}}{R_1 R_N} & \frac{1}{2R_1\sqrt{\bar{A_e}}} \\ \frac{\sqrt{\bar{A_e}}}{R_2 R_1} & -\frac{\sqrt{\bar{A_e}}}{R_2^2} & \ldots & \frac{\sqrt{\bar{A_e}}}{R_2 R_N} & \frac{1}{2R_2\sqrt{\bar{A_e}}} \\ \vdots & \vdots & \ddots & \vdots & \vdots \\ \frac{\sqrt{\bar{A_e}}}{R_N R_1} & \frac{\sqrt{\bar{A_e}}}{R_N R_2} & \ldots & -\frac{\sqrt{\bar{A_e}}}{R_N^2} & \frac{1}{2R_N\sqrt{\bar{A_e}}} \end{bmatrix}. \tag{16}$$

Therefore, the minimization of $\mathcal{L}(\mathbf{u})$ can be replaced with the minimization of the following quadratic form [20, 21],

$$\mathcal{L}^{'} = \frac{1}{2}\mathbf{x}\mathbf{A}\mathbf{x}^T - \mathbf{b}\mathbf{x}, \tag{17}$$

where,

$$\mathbf{x} = \mathbf{u} - \mathbf{u}_0; \tag{18}$$

$$\mathbf{A} = \mathbf{\Sigma}^{-1} - \frac{\mathbf{D}\mathbf{D}^T}{\sigma^2}; \text{and} \tag{19}$$

$$\mathbf{b} = \mathbf{D}\frac{\left(\mathbf{m}(\mathbf{u}) - \hat{\mathbf{m}}(\mathbf{u})\right)}{\sigma^2} + \mathbf{\Sigma}^{-1}\mathbf{u}_0, \tag{20}$$

where $\mathbf{m}(\mathbf{u})$ is the vector of all differential measurements dM_i stacked together. Here, the matrix $\mathbf{A}$ is the Hessian matrix of the quadratic form and the vector $\mathbf{b}$ is the gradient of $\mathcal{L}^{'}$ computed at the current estimate. We search for the minimum in $\mathbf{x}$ in using a conjugate gradient method. At the minimum, we update the current estimate $\mathbf{u} = \mathbf{u}_0 + \mathbf{x}$, recompute $\hat{\mathbf{m}}(\mathbf{u})$ and $\mathbf{D}$, and repeat the minimization procedure iteratively until the current estimate converges. Therefore, finding the MAP estimate requires rendering the signal strength magnitude and compute the derivatives for any values of the model parameters.

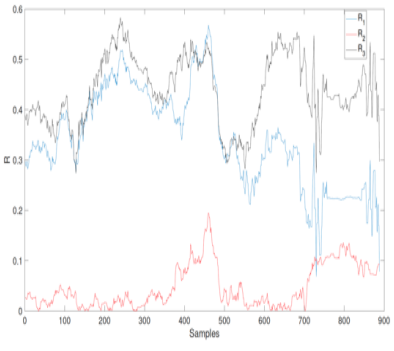

Fig. 3. Distances from the three APs in meters.

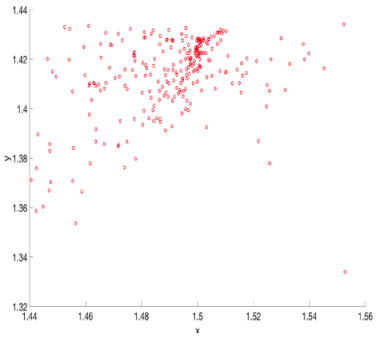

Fig. 4. (x, y) positions in meters.

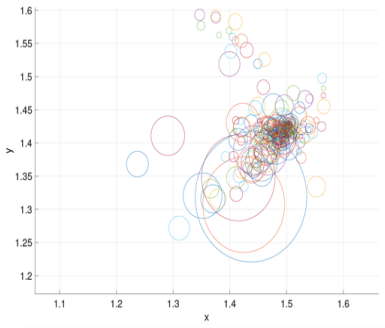

Fig. 5. Point spread function in meters.

After estimating the vector $\mathbf{u}$, the last entry represents the estimate of the effective moving surface area, while the first N entries of the vector $\mathbf{u}$ represent the estimated distances to each AP, which will be used to infer the position and the velocity of the moving surface as follows. Once again, using Bayes theorem [26], we have

$$p(x, y, z, s|\mathbf{u}) \propto p(\mathbf{u}|x, y, z, s)p(x, y, z, s), \qquad (21)$$

where (x, y, z) is the position of the moving surface and s is a scale. We follow the same procedure conducted in Equations (9) through (11), where the prior here is assumed to be inverse Gaussian distribution [28], as it fits with the beamforming nature of the wireless radios.

The position of the moving surface and the scale are estimated by solving the following set of N quadratic equations,

$$(x-x_i)^2+(y-y_i)^2+(z-z_i)^2 = sR_i^2, \quad i = 1, \ldots, N. \quad (22)$$

The method of choice is Levenberg–Marquardt minimization [29]. The corresponding velocities are estimated as follows,

$$v_{x_i}^2 + v_{y_i}^2 + v_{z_i}^2 = \left(\frac{\frac{\lambda}{4\pi} d\phi_{t,t-1}}{dt} \right)_i^2, \quad i = 1, \ldots, N, \quad (23)$$

where, t is the time index.

For estimation in 2D space, $N \geq 3$, because one needs at least three access points to form a plane. For estimation in 3D space, $N \geq 4$, because one needs at least two planes to make inference in 3D space.

IV. Preliminary Numerical Results

In our experiments, the CSI is collected from Cisco 4800 WiFi APs (Cisco Systems Inc., San Jose, CA, USA) on the 5 GHz radio frequency for WiFi. We use three APs for 2D inference. The three APs are placed to form a triangle, and they are put on desks. The first AP is assumed to be the origin. The second AP is aligned with the first AP in the y direction, and is located two meters away from the first AP in the x direction. The third AP is located two meters away from the first AP in each of the and x and y directions. The client is a fixed device pinging the three APs at an interval with a mean two milliseconds and a variance of one millisecond. The received CSI information is filtered on the mac address of the client. People were moving casually around the three APs.

Micro-motions estimates generate dense distributions. We provide sample snapshot of the used CSI. The probabilistic results of the distances-from-APs estimates, positions in the x and y directions and effective surface area are provided.

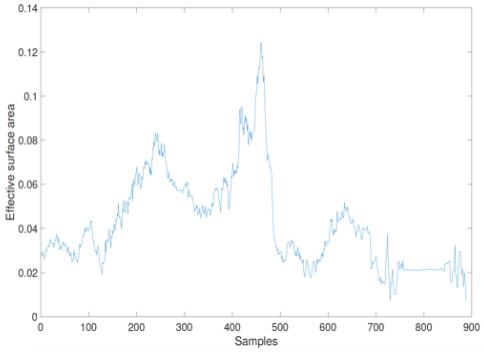

Fig. 6. Effective surface area of the moving surface in m^2.

We also present numerical estimations for the point spread function from the statistics of the surface location.

Fig. 3 shows the estimated distances from the effective moving surface to each of the three APs. Based on these distances, the system of equations given in (22) is solved to infer the locations, and these locations are pictorially shown in Fig. 4. A scale of 9.1 is inferred.

Fig. 5 shows the point spread function for each of the inferred points (shown in Fig. 4) via a 50-standard-deviations window of the three estimated distances, which shows how the motions are statistically spread out around the inferred location, at every time instance. Finally, Fig. 6 shows the effective surface area of the moving surface versus samples. The effective surface area reflects how big the moving surface is. Extensive testing results will be provided in an extended publication, where automation and dedicated control environments will be considered.

V. Conclusions

In this paper, a general inference framework has been proposed for the tracking of general moving micro surfaces, where the model choice is determined by the natural and physical properties of the surface we infer. Bayesian inference is formulated, and a combination of gradient descent and Levenberg–Marquardt algorithms is conducted. For the case of radio signals collected from Cisco wireless 4800 access points, we provided estimates of the moving micro surface area and locations, as well as velocities, based on the proposed model.

REFERENCES

[1] C.-S. Yang, P. Tsai, M. Liao, C. Huang, and C. Yeh, "Location-based mobile multimedia push system," in *Proceedings - 2010 International Conference on Cyber-Enabled Distributed Computing and Knowledge Discovery, CyberC 2010*, pp. 181–184, November 2010.

[2] J. Yim, S. Ganesan, and B. Kang, "Location-based mobile marketing innovations," *Mobile Information Systems*, vol. 2017, pp. 1–3, October 2017.

[3] L. Wu and M. Stilwell, "Exploring the marketing potential of location-based mobile games," *Journal of Research in Interactive Marketing*, vol. 12, December 2017.

[4] S. Y. Carrizales-Villagómez, M. A. Nuño-Maganda, and J. Rubio-Loyola, "A platform for e-health control and location services for wandering patients," *Mobile Information Systems*, vol. 2018, pp. 8164376:1–8164376:18, April 2018.

[5] A. Yassin, Y. Nasser, M. Awad, A. Al-Dubai, R. Liu, C. Yuen, R. Raulefs, and E. Aboutanios, "Recent advances in indoor localization: A survey on theoretical approaches and applications," *IEEE Communications Surveys Tutorials*, vol. 19, pp. 1327–1346, November 2016.

[6] R. Brena, J. García-Vázquez, C. Galván Tejada, D. Munoz, C. Vargas-Rosales, J. Fangmeyer Jr, and A. Palma, "Evolution of indoor positioning technologies: A survey," *Journal of Sensors*, vol. 2017, March 2017.

[7] D. Wang and M. Fattouche, "OFDM transmission for time-based range estimation," *IEEE Signal Processing Letters*, vol. 17, pp. 571–574, June 2010.

[8] G. Zhao, D. Wang, and M. Fattouche, "Time sum of arrival based BLUE for mobile target positioning," *Advanced Science Letters*, vol. 4, pp. 165–167, January 2011.

[9] H. Nurminen, M. Dashti, and R. Piché, "A survey on wireless transmitter localization using signal strength measurements," *Wireless Communications and Mobile Computing*, vol. 2017, pp. 1–12, February 2017.

[10] H. Zhu and T. Alsharari, "An improved RSSI-based positioning method using sector transmission model and distance optimization technique," *International Journal of Distributed Sensor Networks*, vol. 2015, September 2015.

[11] M. Passafiume, S. Maddio, and A. Cidronali, "An improved approach for RSSI-based only calibration-free real-time indoor localization on IEEE 802.11 and 802.15.4 wireless networks," *Sensors*, vol. 17, March 2017.

[12] Y. Zhuang, J. Yang, Y. Li, L. Qi, and N. El-Sheimy, "Smartphone-based indoor localization with Bluetooth low energy beacons," *Sensors*, vol. 16, p. 596, April 2016.

[13] Z. Jia, C. Wu, Z. Li, Y. Zhang, and B. Guan, "The indoor localization and tracking estimation method of mobile targets in three-dimensional wireless sensor networks," *Sensors*, vol. 15, pp. 29661–29684, November 2015.

[14] X. Wang, L. Gao, S. Mao, and S. Pandey, "CSI-based fingerprinting for indoor localization: A deep learning approach," *IEEE Transactions on Vehicular Technology*, vol. 66, pp. 763–776, January 2017.

[15] P. Xiang, P. Ji, and D. Zhang, "Enhance RSS-based indoor localization accuracy by leveraging environmental physical features," *Wireless Communications and Mobile Computing*, vol. 2018, pp. 1–8, July 2018.

[16] A. Ahmed, R. Arablouei, F. Hoog, B. Kusy, R. Jurdak, and N. Bergmann, "Estimating angle-of-arrival and time-of-flight for multipath components using WiFi channel state information," *Sensors*, vol. 18, p. 1753, May 2018.

[17] Z. Yang, Z. Zhou, and Y. Liu, "From RSSI to CSI: Indoor localization via channel response," *ACM Comput. Surv.*, vol. 46, December 2013.

[18] T. Konishi, T. Kubo, K. Watanabe, and K. Ikeda, "Variational Bayesian inference algorithms for infinite relational model of network data," *IEEE Transactions on Neural Networks and Learning Systems*, vol. 26, pp. 2176–2181, September 2015.

[19] D. S. Xue and M. S. Si, "Bayesian inference approach to particle size distribution estimation in ferrofluids," *IEEE Transactions on Magnetics*, vol. 42, pp. 3657–3660, November 2006.

[20] R. D. Morris, P. Cheeseman, V. N. Smelyanskiy, and D. A. Maluf, "A Bayesian approach to high resolution 3D surface reconstruction from multiple images," in *Proceedings of the IEEE Signal Processing Workshop on Higher-Order Statistics. SPW-HOS '99*, pp. 140–143, June 1999.

[21] V. N. Smelyanskiy, P. Cheeseman, D. A. Maluf, and R. D. Morris, "Bayesian super-resolved surface reconstruction from images," in *Proceedings IEEE Conference on Computer Vision and Pattern Recognition. CVPR 2000 (Cat. No.PR00662)*, vol. 1, pp. 375–382 vol.1, June 2000.

[22] P.-P. Sloan, J. Kautz, and J. Snyder, "Precomputed radiance transfer for real-time rendering in dynamic, low-frequency lighting environments," *ACM Trans. Graph.*, vol. 21, p. 527–536, July 2002.

[23] K. Hara, K. Nishino, and K. lkeuchi, "Light source position and reflectance estimation from a single view without the distant illumination assumption," *IEEE Transactions on Pattern Analysis and Machine Intelligence*, vol. 27, pp. 493–505, April 2005.

[24] A. F. Molisch, *Wireless Communications*. Wiley Publishing, 2nd ed., 2011.

[25] D. M. Pozar, *Microwave engineering; 3rd ed.* Hoboken, NJ: Wiley, 2005.

[26] A. Leon-Garcia, *Probability, Statistics, and Random Processes for Electrical Engineering*. Upper Saddle River, NJ: Pearson/Prentice Hall, third ed., 2008.

[27] S. Boyd and L. Vandenberghe, *Convex Optimization*. USA: Cambridge University Press, 2004.

[28] K. Gillen-Christandl, G. D. Gillen, M. J. Piotrowicz, and M. Saffman, "Comparison of Gaussian and super Gaussian laser beams for addressing atomic qubits," *Applied Physics B*, vol. 122, April 2016.

[29] K. Levenberg, "A method for the solution of certain non–linear problems in least squares," 1944.